

Space Velocities of L- and T-type Dwarfs

M. R. Zapatero Osorio, E. L. Martín¹ and V. J. S. Béjar
Instituto de Astrofísica de Canarias, E-38205 La Laguna, Tenerife, Spain
 mosorio,ege,vbejar@iac.es

H. Bouy²
University of California at Berkeley, Astronomy Dept., 601 Campbell Hall, Berkeley CA 94720, USA
 hbouy@astro.berkele.edu

R. Deshpande
University of Central Florida, Department of Physics, P.O. Box 162385, Orlando, FL 32816-2385, USA
 rohit@physics.ucf.edu
 and

R. J. Wainscoat
Institute for Astronomy, 2680 Woodlawn Drive, Honolulu, HI 96822, USA
 rjw@ifa.hawaii.edu

ABSTRACT

We have obtained radial velocities of a sample of 18 ultracool dwarfs with spectral types in the interval M6.5–T8 using high-resolution, near-infrared spectra obtained with NIRSPEC and the Keck II telescope. Among our targets there are two likely field stars of type late M, one M6.5 Pleiades brown dwarf, and fifteen L and T likely brown dwarfs of the solar neighborhood with estimated masses in the range 30–75 M_{Jup} . Two dwarfs, vB 10 (M8V) and Gl 570 D (T7.5V/T8V), are known wide companions to low-mass stars. We have confirmed that the radial velocity of Gl 570 D is coincident with that of the K-type primary star Gl 570 A, thus providing additional support for their true companionship. The presence of planetary-mass companions around 2MASS J05591914–1404488 (T4.5V) has been analyzed using five NIRSPEC radial velocity measurements obtained over a period of 4.37 yr. Using our radial velocity data and the radial velocities of an additional set of eight L-type dwarfs compiled from the literature in combination with their proper motions and trigonometric parallaxes, we have computed UVW space motions for the complete expanded sample, which comprises a total of 21 L and T dwarfs within 20 pc of the Sun. This ultracool dwarf population shows UVW velocities that nicely overlap the typical kinematics of solar to M-type stars within the same spatial volume. However, the mean Galactic ($v_{\text{tot}} = 44.2 \text{ km s}^{-1}$) and tangential ($v_t = 36.5 \text{ km s}^{-1}$) velocities of the L and T dwarfs appear to be smaller than those of G to M stars. A significant fraction ($\sim 40\%$) of the L and T dwarfs lies near the Hyades moving group (0.4–2 Gyr), which contrasts with the 10–12% found

¹Also at University of Central Florida, Dept. of Physics, P. O. 162385, Orlando FL 32816-2385, USA

¹Also at Instituto de Astrofísica de Canarias, E-38205 La Laguna, Tenerife, Spain

for earlier-type stellar neighbors. Additionally, the distributions of all three UVW components ($\sigma_{UVW} = 30.2, 16.5, 15.8 \text{ km s}^{-1}$) and the distributions of the total Galactic ($\sigma_{v_{\text{tot}}} = 19.1 \text{ km s}^{-1}$) and tangential ($\sigma_{v_t} = 17.6 \text{ km s}^{-1}$) velocities derived for the L and T dwarf sample are narrower than those measured for nearby G, K, and M-type stars, but similar to the dispersions obtained for F stars. This suggests that, in the solar neighborhood, the L- and T-type ultracool dwarfs in our sample (including brown dwarfs) is kinematically younger than solar-type to early M stars with likely ages in the interval 0.5–4 Gyr.

Subject headings: stars: low-mass, brown dwarfs — stars: kinematics — stars: late-type

1. Introduction

L- and T-type dwarfs are very cool ($T_{\text{eff}} \leq 2200 \text{ K}$), intrinsically faint objects of recent discovery (e.g., Nakajima et al. 1995; Ruiz et al. 1997; Delfosse et al. 1997; Martín et al. 1997; see review by Kirkpatrick 2005), which are frequently referred to as “ultracool” dwarfs. Over 500 of these ultracool objects have been identified to date. Many of them are found isolated in the solar neighborhood, i.e., within 50 pc of the Sun; only a few appear as widely separated ($a \geq 10 \text{ AU}$) companions to stars (e.g., Nakajima et al. 1995; Rebolo et al. 1998; Burgasser et al. 2000; Kirkpatrick et al. 2001; Liu et al. 2002; Potter et al. 2002; Metchev & Hillenbrand 2004) and as tight stellar companions (Freed et al. 2003). Yet their physical and kinematic properties are not fully known. According to theoretical evolutionary models (e.g., Burrows et al. 1997; Chabrier & Baraffe 2000), the late L and T dwarfs of the solar neighborhood are brown dwarfs with likely substellar masses in the range 0.03–0.075 M_{\odot} .

The detailed studies of low-resolution spectra and color–magnitude diagrams of L and T dwarfs (e.g., Leggett et al. 2002; Patten et al. 2006; Kirkpatrick et al. 1999; Martín et al. 1999; Geballe et al. 2002; Burgasser et al. 2002) are beginning to shed light on the physical characteristics of these low-mass objects because an increasing number of trigonometric parallaxes (distances) have been determined for field ultracool dwarfs (Dahn et al. 2002; Tinney et al. 2003; Vrba et al. 2004; Knapp et al. 2004). Besides distance and proper motion, the additional ingredient for a complete kinematic study employing space velocity components is radial velocity. Reid et al. (2002), Mohanty & Basri (2003) and Bailer-Jones (2004) have obtained the first radial velocity measurements available for L-type dwarfs in the solar vicinity using high-resolution optical spectra. The

marked low luminosities of the T dwarfs prevent accurate velocity determination at visible wavelengths.

Therefore, interpretation of the kinematics of the least massive (including the substellar) population of the solar vicinity is less developed than in the case of stars. Various groups have investigated the dynamics and age of the Galactic disk by examining the observed and simulated kinematics of nearby stars (e.g., Nordström et al. 2004, and references therein). It is found that the space velocity dispersion of stars increases with time to the α power (t^{α}) with $\alpha = 0.33$ (Binney et al. 2000). Statistically, most solar-type to early M stars within 50 pc of the Sun show kinematic ages very similar to the age of our solar system at about 5 Gyr. A small fraction of these stars turn out to be members of stellar moving groups characterized by much younger ages from a few hundred megayears to a few gigayears (Zuckerman & Song 2004). However, the nearby, coolest M dwarfs appear to behave differently. As noted by Reid et al. (2002) and Dahn et al. (2002), their kinematics suggest that the latest M stars of the solar neighborhood are on average younger than earlier-type stars.

Here, we report on radial velocity measurements of ultracool L and T dwarfs obtained from near-infrared spectra (Section 2). Radial velocity variability has been investigated for a few targets in Section 3. These data have been combined with trigonometric parallaxes and proper motions published in the literature to derive galactic velocities in Section 4. Our final remarks and conclusions are given in Section 5.

2. The sample and observations

The sample of targets is listed in Table 1. It comprises three late M-type dwarfs, one of

which (PP11 or Roque15) is a young, lithium-bearing brown dwarf of the Pleiades cluster (Stauffer et al. 1998). The remaining targets are six L- and nine T-type field dwarfs recently discovered by the 2MASS, SLOAN, and Denis surveys. The discovery papers are all indicated in Table 1 of Zapatero Osorio et al. (2006). The spectral types given in the second column of Table 1 are taken from the literature (Kirkpatrick et al. 1997, 1999, 2000; Martín et al. 1999; Geballe et al. 2002; Burgasser et al. 2006; Phan-Bao et al. 2006). They were derived from optical and/or near-infrared low-resolution spectra and are in the interval M6.5–T8. There are objects that have been classified differently by the various groups; we provide all classifications in Table 1, first that of Kirkpatrick et al. (1999) and Burgasser et al. (2006), second that of Geballe et al. (2002), and finally, the classification from Martín et al. (1999). In terms of effective temperature, our sample spans the range 2700–770 K (Leggett et al. 2000; Vrba et al. 2004). J0334–49 and vB 10 can be stars in our sample while the remaining targets are very likely substellar.

We collected high-resolution near-infrared spectra of the 18 ultracool dwarfs using the Keck II telescope and the NIRSPEC instrument, a cross-dispersed, cryogenic echelle spectrometer employing a 1024×1024 ALADDIN InSb array detector. These observations were carried out on different occasions from 2000 December through 2006 January and are part of our large program aimed at the study of radial velocity variability. The complete journal of the observations is shown in Table 1 of Zapatero Osorio et al. (2006), since these data were previously used to determine the rotational velocities of the sample, including the young, lithium-bearing field brown dwarf LP 944–20. We note that the radial velocity of LP 944–20 using NIRSPEC spectra is fully discussed in Martín et al. (2006). In the echelle mode, we selected the NIRSPEC-3 (*J*-band) filter and an entrance slit width of $0''.432$ (i.e., 3 pixels along the dispersion direction of the detector), except for eight targets (J2224–01, J1728+39, J1632+19, J1346–00, J1624+00, J1553+15, J1217–03, and GL 570D) for which we used an entrance slit width of $0''.576$. The length of both slits was $12''$. All observa-

tions were performed at an echelle angle of $\sim 63^\circ$. This instrumental setup provided a wavelength coverage from 1.148 up to $1.346 \mu\text{m}$ split into ten different orders, a nominal dispersion ranging from 0.164 (blue wavelengths) to $0.191 \text{ \AA}/\text{pix}$ (red wavelengths), and a final resolution element of $0.55\text{--}0.70 \text{ \AA}$ at $1.2485 \mu\text{m}$ (roughly the central wavelength of the spectra), corresponding to a resolving power $R \sim 17800\text{--}22700$. Individual exposure times were a function of the brightness of the targets, ranging from 120 to 900 s.

2.1. Data reduction

Raw data were reduced using the ECHELLE package within IRAF¹. Spectra were collected at two or three different positions along the entrance slit. Nodded images were subtracted to remove sky background and dark current. White-light spectra obtained with the same instrumental configuration and for each target were used for flat-fielding the data. All spectra were calibrated in wavelength using the internal arc lamp lines of Ar, Kr, and Xe, which were typically acquired after observing the targets. The vacuum wavelengths of the arc lines were identified and we produced fits using a third-order Legendre polynomial along the dispersion axis and a second-order one perpendicular to it. The mean rms of the fits was 0.03 \AA , or 0.7 km s^{-1} . In order to correct for atmospheric telluric absorptions, near-infrared featureless stars of spectral types A0–A2 were observed several times and at different air masses during the various observing runs. The hydrogen line at $1.282 \mu\text{m}$, which is intrinsic to these hot stars, was removed from the spectra before using them for division into the corresponding science data. Finally, we multiplied the science spectra by the black-body spectrum for the temperature of 9480 K, which is suitable for A0V type (Allen 2000).

We have plotted in Figures 1 to 3 all of our spectra corresponding to the echelle orders centered at $1.230 \mu\text{m}$, the KI doublet ($1.2485 \mu\text{m}$), and $1.292 \mu\text{m}$. These are orders relatively free of strong telluric lines. Effective temperature (i.e.,

¹IRAF is distributed by National Optical Astronomy Observatory, which is operated by the Association of Universities for Research in Astronomy, Inc., under contract with the National Science Foundation.

spectral type) decreases from top to bottom. Note that all spectra have been shifted in velocity to vacuum wavelengths for easy comparison of the atomic and molecular features. The signal-to-noise ratio of the data varies for different echelle orders and different targets depending on their brightness. In general, the red orders show better signal-to-noise ratio than the blue orders, except for the reddest order centered at $1.337\ \mu\text{m}$ in T dwarfs since these wavelengths are affected by strong methane and water vapor absorptions below 1300 K.

2.2. Data analysis: radial velocities

We note that systematic errors or different zero-point shifts may be present in the instrumental wavelength calibration of our data, which may affect the radial velocity measurements. Various authors (Tinney & Reid 1998; Martín 1999; Mohanty & Basri 2003; Basri & Reiners 2006) have reported on the stable heliocentric velocity of the M8V dwarf $\nu\text{B } 10$, finding an average value of $+35.0\ \text{km s}^{-1}$. From our two NIRSPEC spectra and using the centroids of the K I lines, we derived $+35.0$ and $+34.3\ \text{km s}^{-1}$ with an estimated uncertainty of $\pm 1.5\ \text{km s}^{-1}$ associated with each individual determination. These measurements are fully consistent with those in the literature. Furthermore, we have compared NIRSPEC spectra corresponding to echelle orders that contain a considerable number of telluric lines and that were observed during a night and on different nights. We found that the telluric lines typically differ by less than $1\ \text{km s}^{-1}$ in velocity. All this suggests that any systematic errors or different zero-point shifts in our radial velocities are likely smaller than the measurement uncertainties, which are typically $\geq 1\ \text{km s}^{-1}$.

We derived heliocentric radial velocities, v_h , via a cross-correlation of the spectra of our targets against spectra of dwarfs of similar types with known heliocentric velocity. The details of the procedure are fully described in the literature (e.g., Marcy & Benitz 1989). Summarizing, heliocentric radial velocities were obtained from the Doppler shift of the peak of the cross-correlation function between the targets and the templates. To determine the center of the cross-correlation peak we typically fit it with a Gaussian function using the task FXCOR in IRAF. This provides ob-

served velocities that are corrected for the Earth's motions during the observations and converted into heliocentric velocities. Only orders for which we unambiguously identified the peak of the cross-correlation function and obtained good Gaussian fits were employed (see Figure 4 for examples of cross-correlation functions and Gaussian fits). We typically used between 4 and 8 echelle orders depending on the signal-to-noise ratio of the data. All results were then averaged to produce the final v_h measurements. Uncertainties are derived from the standard deviation of the mean.

We used the M8V-type dwarf $\nu\text{B } 10$ as the primary reference/template object for several reasons: first, it is a slow rotator (Mohanty & Basri 2003), thus providing narrow cross-correlation peaks; second, its radial velocity is well determined in the literature to be $+35.0\ \text{km s}^{-1}$; and third, the signal-to-noise ratio of its NIRSPEC spectra is reasonably good (see Figures 1 to 3), minimizing the data noise introduced in the cross-correlation method. This technique assumes that the target and template spectra are of similar type and differ only in the rotation velocity. Nevertheless, Bailer-Jones (2004) has recently shown that M-type templates can also yield accurate velocities for L dwarfs. In our sample, the energy distribution of T dwarfs does differ significantly from M dwarfs, and we found that for the early T-type targets the cross-correlation with $\nu\text{B } 10$ gives reasonable results if the resonance lines of K I are avoided and only molecular (particularly water vapor) lines are used in the cross-correlation. For the late-type objects, cooler templates are required. We employed J2224–01 (L4.5V), J0559–14 (T4.5V), and J1217–03 (T7–8V) as secondary reference dwarfs to obtain the radial velocities of the L- and T-type objects in the sample. Rotation velocities of all targets are provided in column 10 of Table 1 (Zapatero Osorio et al. 2006). The three secondary templates have moderate rotation in the interval $v_{\text{rot}} \sin i = 22\text{--}31\ \text{km s}^{-1}$. However, the derived error bars on radial velocity do not appear to be significantly higher than using the slow rotator $\nu\text{B } 10$, suggesting that, for the spectral resolution and signal-to-noise ratio of our data, radial velocity accuracy shows little dependence on rotation velocity up to $v_{\text{rot}} \sin i \sim 30\ \text{km s}^{-1}$.

Columns 5 through 8 of Table 1 show our measured v_h for all objects observed on different oc-

casions in this program. We also give the observing dates in columns 3 (Universal Time) and 4 (Modified Julian Date). Whenever there is more than one observation available per object, the first spectrum also acts as a template spectrum to obtain radial velocities via the cross-correlation technique, and the derived velocities are provided in column 9 of Table 1. This minimizes the effects of using templates of different spectral types and serves as a test of consistency. Furthermore, such a procedure will allow us to study binarity. Previous radial velocities reported in the literature are listed in the eleventh column of the Table. We note that, with the exception of PP11 (see below), all of our measurements agree with the literature values to within $1\text{-}\sigma$ of the claimed uncertainty.

3. Binarity

G1570D is a known wide companion (~ 1500 AU) to the multiple system G1570ABC (Burgasser et al. 2000). We have determined its heliocentric velocity to be $+28.5 \pm 2.7 \text{ km s}^{-1}$, which is coincident with the radial velocity of the K-type star G1570A ($v_h = +27.0 \pm 0.3 \text{ km s}^{-1}$) as measured by Nidever et al. (2002). This suggests that G1570D is not a short-period binary of mass ratio near 1. The secondary companion, G1570BC, is a spectroscopic binary whose radial velocities span the range $8.8\text{--}37.9 \text{ km s}^{-1}$ (e.g., Marcy & Benitz 1989).

Multiple NIRSPEC spectra obtained on different occasions are available for five dwarfs in our sample. These are shown in Table 2, where we also provide the time elapsed between the first and last observation and the mean heliocentric velocity per object with the associated average error bar. Inspection of all velocities listed in Table 1 reveals no obvious trace of moderate velocity perturbation in any of the dwarfs since all their measured v_h agree within the uncertainties over the time span of the data. This indicates that the dwarfs of Table 2 are not very likely to be close equal-mass binaries.

To relate companion mass to the dispersion of our radial velocities we use the mass function derived from the Keplerian equations (e.g., Marcy & Benitz 1989). The most constraining case in our sample is the T4.5V dwarf J0559–14. For it we can study the presence of planetary-mass companions in short (a few days

or ~ 0.01 AU) and intermediate (a few years or ~ 0.4 AU) orbits. J0559–14 radial velocity curve exhibits $1\text{-}\sigma$ standard deviation of 0.50 km s^{-1} . For a primary mass of about $60 M_{\text{Jup}}$, expected for mid-T field dwarfs with an age of ~ 5 Gyr (Chabrier & Baraffe 2000), and at the $3\text{-}\sigma$ level, companions more massive than $2 M_{\text{Jup}}$ (short periods) and $10 M_{\text{Jup}}$ ($\sim 1\text{-yr}$ period) can be excluded. Figure 5 summarizes these results graphically. The region of parameter space excluded for planets around J0559–14 is comparable to the region excluded around stars. However, because of the time coverage of our observations of J0559–14, we cannot reach firm conclusions on the presence of companions with orbital periods between days and less than a year. Circular orbits have been adopted to compute these estimates. We consider these minimum mass estimates to represent approximate guidelines in future corroborative spectroscopic work.

Regarding J0036+18 and J0539–00, the null detection of radial velocity variations over a few years suggests that no companions of $\sim 10 M_{\text{Jup}}$ or more can exist near them. Similarly, very close-in companions of a few Jupiter masses may be ruled out orbiting PP11 or J0334–49 with a periodicity of a few days. However, we stress that two radial velocity data points constitute statistically too few observations to reach a final conclusion on the presence of Jovian planets around these objects. Further measurements are certainly required to constrain firmly the minimum mass of any possible companion. However, this exercise indicates that companions with masses in the planetary domain lie near the detectability limit in our data.

Interestingly, Martín et al. (1998) measured the heliocentric velocity of the Pleiades brown dwarf PP11 at $+15.4 \pm 1.6 \text{ km s}^{-1}$, which deviates from our measurement (see Table 2) by more than 4σ . Despite the fact that such a difference may suggest the presence of a second object (future observations are pending to test this hypothesis), its total amount seems to be rather large for a planetary companion even though it might account for the peak-to-peak amplitude of the primary radial velocity curve. This may indicate that the companion has a broad orbit and a mass above the deuterium-burning mass limit, i.e., $\geq 13 M_{\text{Jup}}$, thus, it belongs to the brown dwarf

regime. From the locus of PP11 in the K vs $(I - K)$ color-magnitude diagram of the Pleiades cluster, Pinfield et al. (2003) concluded that this object is a probable binary with a mass ratio in the interval $q = 0.75$ – 1 . We note that our NIRSPEC heliocentric velocity of PP11 is fully consistent with the systemic velocity of the Pleiades measured at $+5.4 \pm 0.4 \text{ km s}^{-1}$ (e.g., Liu et al. 1991; Kharchenko et al. 2005), hence providing additional evidence for its membership of this star cluster.

4. Galactic space motions and kinematics

Using our radial velocity measurements and the proper motions and trigonometric parallaxes provided in the literature by Dahn et al. (2002), Vrba et al. (2004), Knapp et al. (2004), and An et al. (2007) we have calculated the U , V , and W heliocentric velocity components in the directions of the Galactic center, Galactic rotation and north galactic pole, respectively, with the formulation developed by Johnson & Soderblom (1987). Note that the right-handed system is employed and that we will not subtract the solar motion from our calculations. The uncertainties associated with each space-velocity component are obtained from the observational quantities and their error bars after the prescriptions of Johnson & Soderblom (1987). Our derivations are shown in Table 3. Unfortunately, two T dwarfs in the sample lack distance and proper motion measurements, thus preventing us from determining their Galactic velocities (these dwarfs are not shown in Table 3). No trigonometric parallaxes are available for PP11 and the M9V dwarf J0334–49; we have adopted the Pleiades distance for the former object (An et al. 2007) and the poorly constrained spectroscopic distance estimate of Phan-Bao et al. (2006) for the latter, which result in relatively large uncertainties associated with the derived UVW velocities.

With the only exceptions of PP11 and J1728+39AB, the remaining objects in our sample with known trigonometric parallax lie within 20 pc of the Sun. To carry out a reliable statistical study of the kinematics of the least massive population in the solar neighborhood, we have enlarged our sample of ultracool dwarfs with an additional set of eight L-type objects of known trigonometric dis-

tance ($d \leq 20 \text{ pc}$), proper motion and radial velocity (Dahn et al. 2002; Mohanty & Basri 2003; Bailer-Jones 2004; Vrba et al. 2004). This additional set is shown in Table 4, where we also provide our UVW computations obtained in the manner previously described. Hence, UVW space velocities are finally available for a total of 21 L and T dwarfs located at less than $\sim 20 \text{ pc}$ from the Sun.

4.1. Star moving groups

For the following discussion, we will focus on the extended sample of L and T dwarfs. Their Galactic motions are depicted in the UV and VW planes in Fig. 6. As can be seen from the top panels, the space velocities of most L and T dwarfs appear to be rather scattered in these diagrams, and no preferred region (or clustering) of high density and small velocity dispersion is perceptible. Leggett (1992) summarized the criteria used for kinematically classifying old/young disk and halo stars as follows: objects with $V < -100 \text{ km s}^{-1}$ or high eccentricity in the UV plane are defined to be halo stars; objects with an eccentricity in the UV plane of ~ 0.5 are defined to be old disk-halo stars; objects with $-50 < U < +20$, $-30 < V < 0$, and $-25 < W < +10 \text{ km s}^{-1}$ (i.e., the “young disk” ellipsoid) are defined to be young disk sources. Stars that lie outside this ellipsoid are defined to be old disk or young-old disk objects depending on their W velocity. Employing these criteria and from the inspection of the UVW velocities, none of the L and T dwarfs in our study seems to belong to the old-disk or halo kinematic categories; all of them can actually be grouped into the young disk and young-old disk kinematic classifications, suggesting that they are likely objects with ages typical of the solar system and younger.

To further develop this idea, we have superimposed in the bottom panels of Fig. 6 the location of known, nearby star moving groups (streams of stars with common motion through the Milky Way). The UVW velocities and their associated $1\text{-}\sigma$ velocity dispersions used to depict the ellipsoids of the various moving groups shown in Fig. 6 are taken from the literature (Eggen 1992; Chen et al. 1997; Dehnen 1998; Chereul et al. 1999; Montes et al. 2001; Zuckerman & Song 2004; Famaey et al. 2005; Zuckerman et al. 2006). Ordered by increas-

ing age, the β Pictoris (10–30 Myr), AB Dor (\sim 50 Myr), Carina-near (\sim 200 Myr), Ursa Majoris (\sim 300 Myr), and Hyades (0.4–2 Gyr) moving groups have been selected for the proximity of all their northern and southern stellar members to the Sun (typically less than 55 pc). The open star cluster Hyades (\sim 625 Myr) lies within the Hyades moving group. Other young moving groups and star clusters of recent discovery are not included in Fig. 6 because they only contain southern stars, like Tucana/Horologium and the TW Hydrae association, or are located farther away, like η Cha and the Pleiades moving group (Zuckerman & Song 2004). The Hyades moving group is the oldest dynamical stream considered in this work, with stellar ages (derived from A–F stars) spanning the interval 400 Myr to \sim 2 Gyr (Chereul et al. 1999), but probably younger than the canonical age of the solar system.

From the bottom *UV*- and *WV*-planes of Fig. 6, it becomes apparent that only three dwarfs in our sample, namely J1624+00 (T6V), J1217–03 (T7V), and J0205–11AB (L7V), all have space velocity components roughly consistent with the Hyades moving group and fall inside the $1.5\text{-}\sigma$ ellipsoid. These are labeled in the bottom panels of Figure 6. We note that J0205–11AB is an equal-mass binary separated by 9.2 AU (Koerner et al. 1999), and that the expected amplitude of the radial velocity curve of each component is therefore less than 3 km s^{-1} for masses below the substellar limit. This has very little impact on the derived *UVW* velocities of J0205–11AB.

Our results for J1624+00, J1217–03, and J0205–11AB are in agreement with the previous work by Bannister & Jameson (2007). These authors also found that J0036+18 (L3.5V/L4V) and J0825+21 (L7.5V) show proper motion consistent with the Hyades moving group; our *UVW* measurements lie close to the $2\text{-}\sigma$ ellipsoid. Bannister & Jameson (2007) also commented on the fact that all these five ultracool dwarfs sit on a very tight sequence in color-magnitude diagrams (suggesting they are coeval objects) consistent with evolutionary models of 500 Myr. Nevertheless, recent works by Famaey et al. (2005) and De Simone et al. (2004) caution against assigning ages based solely on space motion and star moving group memberships. On the contrary, membership in open star clusters provides reliable

age estimates. None of the L and T dwarfs in our sample appears to be unambiguous members of the Hyades star cluster. Recently, Bihain et al. (2006) found that the velocity (or proper motion) dispersion of Pleiades brown dwarfs (\sim 120 Myr) is about a factor of four times higher than that of solar-mass stars in the cluster. In our sample, only J1217–03 has space velocities close to the $4\text{-}\sigma$ ellipsoid centered at $U = -42$, $V = -19$, $W = -1\text{ km s}^{-1}$ (velocity dispersion 0.3 km s^{-1} , De Bruijne et al. 2001), which corresponds to the \sim 625 Myr-old Hyades.

Further study of the bottom *UV*- and *WV*-planes of Fig. 6 reveals that about 40% of the L and T dwarfs lie near the Hyades moving group either within the $2\text{-}\sigma$ ellipsoid or “touching” it (i.e., the error bars cross the $2\text{-}\sigma$ ellipsoid). To analyze the significance of such an apparent concentration, we have collected accurate radial velocities, Hipparcos distances and parallaxes of F-, G-, K- and M-type stars within 20 pc of the Sun from the catalog of Kharchenko (2004). A total of 10 F stars, 25 solar-type stars, 58 K, and 52 early M (M0–M5) stars were selected. Their Galactic *UVW* motions were calculated as for our L–T sample contained within the same spatial volume. The left panels of Fig. 7 show the space velocities of these stars and of our extended sample as a function of heliocentric distance.

After inspection of the space velocity distribution of the G to early M stars in the *UV*- and *WV*-planes, we found that only 10–12% of the stars (very similar statistics for all three stellar spectral types) lie within or in the “surroundings” of the Hyades moving group, which contrasts with the higher value, 40%, derived for the ultracool dwarfs. Furthermore, under the assumption that the L–T population follows a Poissonian distribution with the same object density than the G to early-M stars, we have estimated the probability of finding eight out of 21 (\sim 40%) ultracool dwarfs close to the Hyades moving group to be lower than 1%, indicating that this concentration is significant to a confidence level of about 99%. This suggests that, on average, the L and T population is kinematically younger than the majority of the stars in the solar neighborhood.

4.2. Galactic kinematics and age of the ultracool dwarfs

From the left panels of Fig. 7 it is evident that the UVW components of the L and T dwarfs overlap the range of space velocities observed for the G, K, and early M stars, i.e., they are neither larger nor dramatically smaller despite the reduced mass of the L- and T-type objects. We can discuss this further by producing the histograms shown in the middle panels of Fig. 7, which depict the UVW distributions for the three populations (K-type stars, early M stars, and the L and T ultracool dwarfs). The cumulative distributions are displayed in the right-most panels of Fig. 7. We can compare these distributions quantitatively using the Kolmogorov–Smirnov test. Such comparison globally shows that there is a probability of more than 15% that the ultracool dwarfs and the K and M0–M5 stars are drawn from the same kinematic population. While this holds for a comparison between the U and W velocity dispersions of the L–T dwarfs and the K–M stellar samples, the test suggests larger differences for the V distributions (galactic rotation) of the K-type stars and the ultracool dwarfs; however, these differences are not statistically meaningful and we will not discuss them further.

In addition, the width of the histograms of Fig. 7, represented by the parameters $\sigma_U, \sigma_V, \sigma_W$, is relevant for a complete kinematic analysis. It is well established that all three velocity dispersions increase with age (Spitzer & Schwarzschild 1951; Mayor 1974; Wielen 1977). We have obtained σ_U, σ_V , and σ_W for each stellar and substellar populations (see Table 5). The Galactic motion dispersions of the G- to M5-type stars are in full agreement with the values obtained for the thin disk of the Galaxy available in the literature (e.g., Hawley et al. 1996; Bensby et al. 2003), even though all these works include a larger number of stars and volumes in their studies. All the L and T dwarfs in our sample have typical perpendicular distances to the Galactic plane in the interval ± 15 pc. Our σ_U and σ_W derivations for the F-type stars also coincide with the literature; however, the derived σ_V value appears smaller than the 20 km s^{-1} found for the thin disk A and F stars by Bensby et al. (2003). This could be explained as statistical noise due to the relative small number (10) of F stars in our study.

We have found that the Galactic velocity distributions corresponding to the ultracool L–T dwarfs are narrower (i.e., lower dispersions in all three space velocities) than those of G to M5 stars. However, our derived σ_U, σ_V , and σ_W for the L–T dwarfs are remarkably similar to results obtained for M-type emission-line stars (e.g., Hawley et al. 1996) and very active M7-type stars (West et al. 2006), which are generally assigned ages of less than ~ 3 Gyr (Reid et al. 2002). We also note that if the $\sim 40\%$ of the L and T dwarfs lying within and near the Hyades moving group in the UVW planes is removed from the statistical analysis, the three parameters σ_U, σ_V , and σ_W will gently increase; nevertheless, they remain smaller than the Galactic velocity dispersions observed for solar to early-M stars. Interestingly, all three σ_{UVW} of L and T dwarfs resemble the velocity dispersions of F-type stars (Table 5), suggesting that the two populations (despite their very different mass) share similar ages on average.

There are various empirical calibrations of the relationship between velocity dispersion, particularly σ_W , and age (Mayor 1974; Haywood et al. 1997; e.g., Nordström et al. 2004, and references therein) that we can use to estimate the mean age for our kinematic samples. According to the σ -age relations provided in Tables 2 (A and F stars) and 3 (G–K–M stars) by Mayor (1974), the mean age of the 20-pc sample of F stars is about 2 Gyr, and that of the G to early M stars is about 5 Gyr (i.e., the age of the Sun). Wielen (1977) published a mathematical relation between age and the dispersion of the total Galactic velocity (see also Schmidt et al. (2007)). We have computed the mean Galactic velocity, $\langle v_{\text{tot}} \rangle$, and its associated dispersion, $\sigma_{v_{\text{tot}}}$, for all spectral types listed in Table 5. Galactic velocities comprise the three components of the space velocities and as such, may summarize the statistical effects seen in each velocity component (unless they are canceled out). The kinematical ages derived from Wielen (1977) equation are also provided in the Table. The L–T population shows a kinematical age in the range 0.5–2.3 Gyr; it thus appears to be a factor of two younger than the low-mass stars of the solar neighborhood. From the analysis of the tangential velocities of a sample of late M and L dwarfs, Dahn et al. (2002) and Schmidt et al. (2007) also concluded that these objects have a mean age of

2–4 Gyr, consistent with our derivation. The fact that the late M-type stars of the solar vicinity appear to be younger, on average, than earlier-type stars was previously suggested in the literature (Hawkins & Bessell 1988; Kirkpatrick et al. 1994; Reid et al. 1994, 2002). Here, we extend this result to the coolest spectral types (L and T) including the brown dwarf population.

Finally, various groups have also pointed out that nearby, very low-mass stars tend to have smaller space motions compared to the earlier-type stars, although the difference is claimed to be of marginal significance (Reid et al. 2002; Dahn et al. 2002). We provide in Table 5 the average proper motion, $\langle \mu \rangle$, for the F, G, K, M0–M5, L and T dwarf populations with known trigonometric parallaxes considered in this work (1- σ dispersions are given in brackets). Nevertheless, the information on the mean distance and the mean proper motion is better encapsulated in the mean tangential velocity, $\langle v_t \rangle$, which we also provide in Table 5. To complete the spectral sampling between the early M stars and the ultracool dwarfs of our study we have collected the *UVW* data of 29 M6–M9 objects at less than 23 pc of the Sun from Table 5 of Reid et al. (2002). These authors obtained accurate radial velocities for these objects and combined them with astrometric proper motions and photometric parallaxes to compute Galactic velocities. We show in Table 5 our derivation of $\sigma_U, \sigma_V, \sigma_W$, and the mean Galactic velocity, proper motion, and tangential velocity for the reduced sample of M6–M9 objects extracted from Reid et al. (2002).

Figure 8 illustrates the dependence of $\langle v_{\text{tot}} \rangle$, $\langle v_t \rangle$ and their associated dispersions ($\sigma_{v_{\text{tot}}}, \sigma_{v_t}$) on spectral type (or mass). We note that the values corresponding to the F-type stars have less statistical weight because they have been derived from a low number of objects. After comparison with the literature values, the Galactic velocity dispersion $\sigma_{v_{\text{tot}}}$ of F stars shown in Table 5 is likely to be increased by a few km s^{-1} . The diagrams of Fig. 8 (which do not incorporate this correction) cover a wide range of masses, from $\sim 2 M_\odot$ (F-type stars) down to $\sim 50 M_{\text{Jup}}$ (or $0.05 M_\odot$, T-types). Note that we have split our full sample of ultracool dwarfs into the two L and T types. As seen in the right panels of Fig. 8, K-type stars display the largest mean Galactic and tangential veloci-

ties, while F stars and the ultracool dwarfs have smaller values. We note that the mean velocities of M6–M9 stars are comparable to those of the ultracool L and T dwarfs, in perfect agreement with the results obtained for late-M and L-type objects by Schmidt et al. (2007).

The $\sigma_{v_{\text{tot}}}$ - and σ_{v_t} -spectral type relations shown in the right panels of Fig. 8 present similar structure: an increasing trend from F to K stars to decrease at cooler types; the L and T population displays the smallest velocity dispersions. We ascribe this behavior to the likely younger kinematical ages of the ultracool and very low-mass objects in the solar neighborhood. There is a hint in our data suggesting that T dwarfs are slightly younger than L dwarfs; further observations and larger samples are required to confirm it. This result may be affected by an observational bias in the way L and T dwarfs are discovered. Since brown dwarfs cool down and grow fainter with age, it is expected that magnitude-limited surveys would find younger objects in general. However, according to state-of-the-art evolutionary model predictions on substellar temperatures and luminosities and the fact that our study is limited to a distance of 20–23 pc, this bias is not largely contaminating our sample of ultracool dwarfs. Any model explaining the population of the Galaxy should account for the relations shown in Fig. 8 quantitatively, which may provide a constraint on the field mass function and the stellar/substellar formation rate.

5. Conclusions

Radial velocities have been obtained for a sample of 18 M6.5–T8 dwarfs using high-resolution ($R = 17800\text{--}22700$), near-infrared ($1.148\text{--}1.346 \mu\text{m}$) spectra collected with the NIRSPEC instrument on the Keck II telescope. The sample comprises one M6.5 Pleiades brown dwarf, two late-M field dwarfs, and 15 L and T likely brown dwarfs of the solar neighborhood with masses in the range $30\text{--}75 M_{\text{Jup}}$. Our radial velocity measurements further confirm the membership of PP11 in the Pleiades cluster, and the true physical companionship of the T7.5V/T8V G1570D dwarf in the G1570 multiple system. From five velocity measurements obtained for 2MASS J05591914–1404488 (T4.5V) over 4.37 yr

and the observed velocity dispersion of 0.5 km s^{-1} , we discard the possible presence of massive jovian planets near this brown dwarf with orbits of a few days or around a year.

All the L and T dwarfs in our sample lie ≤ 24 pc from the Sun, and trigonometric parallaxes and proper motions are available for nearly all of them from Dahn et al. (2002), Vrba et al. (2004), and Knapp et al. (2004). We have used our radial velocity determinations and astrometric data from the literature to derive Galactic UVW velocities. The total number of ultracool dwarfs within 20 pc of the Sun is augmented up to 21 with the addition of eight L dwarfs of known trigonometric distance, proper motion and radial velocity available in the literature. We have compared the Galactic and tangential velocities of the ultracool dwarf population to those of F, G, K, and M stars contained in the same volumen. The UVW distributions of the complete expanded L and T sample show a smaller dispersion than the G to M stars and a comparable dispersion to the F-type stars. Similar behavior is observed for the total Galactic velocity and tangential velocity dispersions, suggesting that the least massive population, which includes brown dwarfs, is kinematically younger. Furthermore, we find that a significant fraction ($\sim 40\%$) of the L and T dwarfs in our sample lies near the location of the Hyades moving group in the UV and VW planes in contrast to the low rate (10–12%) observed for stars. This, in addition to the lower dispersions observed in all space velocities, suggests that our sample of L and T dwarfs (many are brown dwarfs) is kinematically young with likely ages below 5 Gyr.

We thank the referee for useful comments. The data were obtained at the W. M. Keck Observatory, which is operated as a scientific partnership between the California Institute of Technology, the University of California, and NASA. The Observatory was made possible by the generous financial support of the W. M. Keck Foundation. The authors extend special thanks to those of Hawaiian ancestry on whose sacred mountain we are privileged to be guests. We thank the Keck observing assistants and the staff in Waimea for their kind support. This research has made use of the SIMBAD database, operated at CDS, Strasbourg, France, and has been supported by a Keck PI Data

Analysis grant awarded to E. L. M. by Michelson Science Center, and by the Spanish projects AYA2003-05355 and AYA2006-12612. We thank Terry Mahoney for his careful reading of the English language. We also thank I. Ribas for early discussions on this topic.

REFERENCES

- Allen, W. B. 2000, *Allen's Astrophysical Quantities*. Fourth edition, ed. Arthur N. Cox, New York: Springer Verlag, p. 151
- An, D., Terndrup, D. M., Pinsonneault, M. H., Paulson, D. B., Hanson, R. B., & Stauffer, J. R. 2007, *ApJ*, 655, 233
- Bailer-Jones, C. A. L. 2004, *A&A*, 419, 703
- Bannister, N. P., & Jameson, R. F. 2007, *MNRAS*, tmp, L44
- Basri, G., & Reiners, A. 2006, *AJ*, 132, 663
- Bensby, T., Feltzing, S., & Lundström, I. 2003, *A&A*, 410, 527
- Bihain, G., Rebolo, R., Béjar, V. J. S., Caballero, J. A., Bailer-Jones, C. A. L., Mundt, R., Acosta-Pulido, J. A., & Manchado Torres, A. 2006, *A&A*, 458, 805
- Binney, J., Dehnen, W., & Bertelli, G. 2000, *MNRAS*, 318, 658
- Burgasser, A. J., Kirkpatrick, J. D., Cutri, R. M., et al. 2000, *ApJ*, 531, L57
- Burgasser, A. J., Adam, J., Kirkpatrick, J. D., et al. 2002, *ApJ*, 564, 421
- Burgasser, A. J., Geballe, T. R., Leggett, S. K., Kirkpatrick, J. D., & Golimowski, D. A. *ApJ*, 637, 1067
- Burrows, A., Marley, M., Hubbard, W. B., et al. 1997, *ApJ*, 491, 856
- Chabrier, G., & Baraffe, I. 2000, *ARA&A*, 38, 337
- Chen, B., Asiain, R., Figueras, F., & Torra, J. 1997, *A&A*, 318, 29
- Chereul, E., Crézé, M., & Bienaymé, O. 1999, *A&ASS*, 135, 5

- Dahn, C. C., et al. 2002, *AJ*, 124, 1170
- Dehnen, W. 1998, *AJ*, 115, 2384
- Delfosse, X., Tinney, C. G., Forveille, T., et al. 1997, *A&A*, 327, L25
- De Bruijne, J. H. J., Hoogerwerf, R., & De Zeeuw, P. T. 2001, *A&A*, 367, 111
- De Simone, R., Wu, X., & Tremaine, S. 2004, *MNRAS*, 350, 627
- Eggen, O. J. 1992, *AJ*, 104, 1482
- Famaey, B., Jorisse, A., Luri, X., Mayor, M., Udry, S., Dejonghe, H., Turon, C. 2001, *A&A*, 430, 165
- Freed, M., Close, L. M., & Siegler, N. 2003, *ApJ*, 584, 453
- Geballe, T. R., Knapp, G. R., Leggett, S. K., et al. 2002, *ApJ*, 564, 466
- Hawkins, M. R. S., & Bessell, M. S. 1988, *MNRAS*, 234, 177
- Hawley, S. L., Gizis, J. E., & Reid, I. N. 1996, *AJ*, 112, 2799
- Haywood, M., Robin, A. C., Creze, M. 1997, *A&A*, 320, 428; 320, 440
- Johnson, D. R. H., & Soderblom, D. R. 1987, *AJ*, 93, 864
- Kharchenko, N. V. 2004, *KFNT*, 20, 366
- Kharchenko, N. V., Piskunov, A. E., Röser, S., Schilbach, E., & Scholz, R.-D. 2005, *A&A*, 438, 1163
- Kirkpatrick, J. D., McGraw, J. T., Hess, T. R., Liebert, J., & McCarthy, D. W. 1994, *ApJS*, 94, 749
- Kirkpatrick, J. D., Henry, T. J., & Irwin, M. J. 1997, *AJ*, 113, 1421
- Kirkpatrick, J. D., Reid, I. N., Liebert, J., et al. 1999, *ApJ*, 519, 802
- Kirkpatrick, J. D., Reid, I. N., Liebert, J., et al. 2000, *AJ*, 120, 447
- Kirkpatrick, J. D., Dahn, C. C., Monet, D. G., Reid, I. N., Gizis, J. E., Liebert, J., & Burgasser, A. J. 2001, *AJ*, 121, 3235
- Kirkpatrick, J. D. 2005, *ARA&A*, 43, 195
- Knapp, G., et al. 2004, *AJ*, 127, 3553
- Koerner, D. W., Kirkpatrick, J. D., McElwain, M. W., & Bonaventura, N. R. 1999, *ApJ*, 526, L25
- Leggett, S. K., Allard, F., Dahn, C., Hauschildt, P. H., Kerr, T. H., & Rayner, J. 2000, *ApJ*, 535, 965
- Leggett, S. K., Golimowski, D. A., Fan, X., et al. 2002, *ApJ*, 564, 452
- Leggett, S. K. 1992, *ApJS*, 82, 351
- Liu, T., Janes, K. A., & Bania, T. M. 1991, *ApJ*, 377, 141
- Liu, M. C., Fischer, D. A., Graham, J. R., Lloyd, J. P., Marcy, G. W., & Butler, R. P. 2002, *ApJ*, 571, 519
- Marcy, G. W., & Benitz, K. J. 1989, *ApJ*, 344, 441
- Martín, E. L. 1999, *MNRAS*, 302, 59
- Martín, E. L., Basri, G., Delfosse, X., & Forveille, T. 1997, *A&A*, 327, L29
- Martín, E. L., Basri, G., Gallegos, J. E., Rebolo, R., Zapatero Osorio, M. R., & Béjar, V. J. S. 1998, *ApJ*, 499, L61
- Martín, E. L., Delfosse, X., Basri, G., Goldman, B., Forveille, T., & Zapatero Osorio, M. R. 1999, *AJ*, 118, 2466
- Martín, E. L., Günther, E., Zapatero Osorio, M. R., Bouy, H., & Wainscoat, R. 2006, *ApJ*, 644, L75
- Mayor, M. 1974, *A&A*, 32, 321
- Metchev, S. A., & Hillenbrand, L. A. 2004, *ApJ*, 617, 1330
- Mohanty, S., & Basri, G. 2003, *ApJ*, 583, 451
- Montes, D., López-Santiago, J., Fernández-Figueroa, M. J., & Gálvez, M. C. 2001, *A&A*, 379, 976

- Nakajima, T., Oppenheimer, B. R., Kulkarni, S. R., Golimowski, D. A., Metthews, K., & Durrance, S. T. 1995, *Nature*, 378, 463
- Nidever, D. K., Marcy, G. W., Butler, R. P., Fischer, D. A., & Vogt, S. S. 2002, *ApJS*, 141, 503
- Nordström, B., Mayor, M., Andersen, J., et al. 2004, *A&A*, 418, 989
- Patten, B. M., Stauffer, J. R., Burrows, A., et al. 2006, *ApJ*, 651, 502
- Perryman, M. A. C., Lindegren, L., Kovalevsky, J. et al. 1997, *A&A*, 323, L49
- Phan-Bao, N., Bessell, M. S., Martín, E. L., et al. 2006, *MNRAS*, 366, L40
- Pinfield, D. J., Dobbie, P. D., Jameson, R. F., Steele, I. A., Jones, H. R. A., & Katsiyannis, A. C. 2003, *MNRAS*, 342, 1241
- Potter, D., Martín, E. L., Cushing, M. C., Baudoz, P., Brandner, W., Guyon, O., Neuhäuser, R. 2002, *ApJ*, 567, L133
- Rebolo, R., Zapatero Osorio, M. R., Madruga, S., Béjar, V. J. S., Arribas, S., Licandro, J. 1998, *Science*, 282, 1309
- Reid, I. N., Tinney, C. G., & Mould, J. 1994, *AJ*, 108, 1456
- Reid, I. N., Kirkpatrick, J. D., Liebert, J., Gizis, J. E., Dahn, C. C., & Monet, D. G. 2002, *AJ*, 124, 519
- Ruiz, M. T., Leggett, S. K., & Allard, F. 1997, *ApJ*, 491, L107
- Schmidt, S. J., Cruz, J. L., Bongiorno, B. J., Liebert, J., & Reid, I. N. 2007, *AJ*, 133, 2258
- Spitzer, L. Jr, & Schwarzschild, M. 1951, *ApJ*, 114, 385
- Stauffer, J. R., Schultz, G., & Kirkpatrick, J. D. 1998, *ApJ*, 499, L199
- Tinney, C. G., & Reid, I. N. 1998, *MNRAS*, 301, 1031
- Tinney, C. G., Burgasser, A. J., Kirkpatrick, J. D. 2003, *AJ*, 126, 975
- Vrba, F. J., Henden, A. A., Luginbuhl, C. B., et al. 2004, *AJ*, 127, 2948
- West, A. A., Bochanski, J. J., Hawley, S. L., Cruz, K. L., Covey, K. R., Silvestri, N. M., Reid, I. N., & Liebert, J. 2006, *AJ*, 132, 2507
- Wielen, R. 1977, *A&A*, 60, 263
- Zapatero Osorio, M. R., Martín, E. L., Bouy, H., Tata, R., Deshpande, R., & Wainscoat, R. J. 2006, *ApJ*, 647, 1405
- Zuckerman, B., & Song, I. 2004, *ARA&A*, 42, 685
- Zuckerman, B., Bessell, M. S., Song, I., & Kim, S. 2006, *ApJ*, 649, L115

This 2-column preprint was prepared with the AAS L^AT_EX macros v5.2.

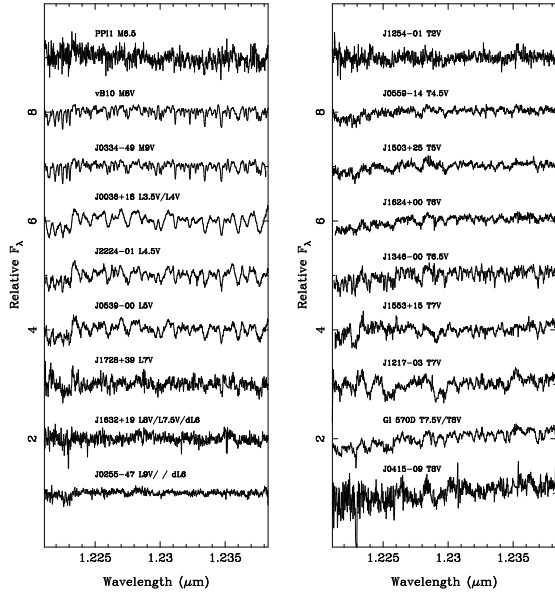


Fig. 1.— NIRSPEC spectra of our sample centered at $1.23 \mu\text{m}$. All spectra are normalized to unity, offset by 1 on the vertical axis, and shifted in velocity to vacuum wavelengths.

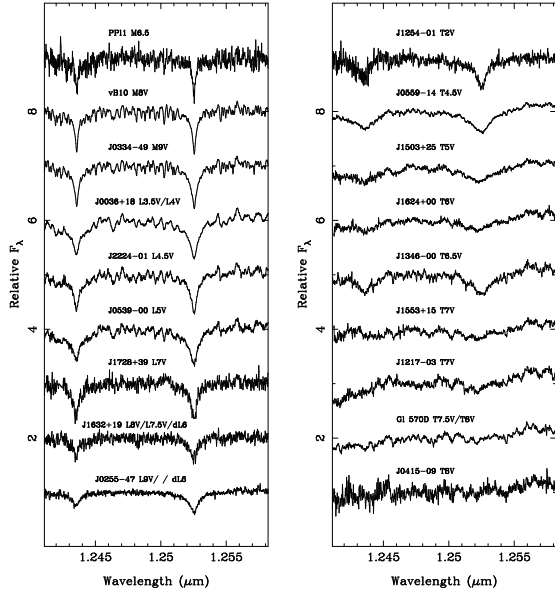


Fig. 2.— NIRSPEC spectra of our sample centered at $1.25 \mu\text{m}$. The most prominent features of the M and L dwarfs are due to KI absorption, which vanishes at late T types. All spectra are offset by 1 on the vertical axis, and shifted in velocity to vacuum wavelengths. Data are normalized to unity in the intervals $1.2465\text{--}1.2475 \mu\text{m}$ (M6.5–T4.5) and $1.2468\text{--}1.2472 \mu\text{m}$ (T5–T8).

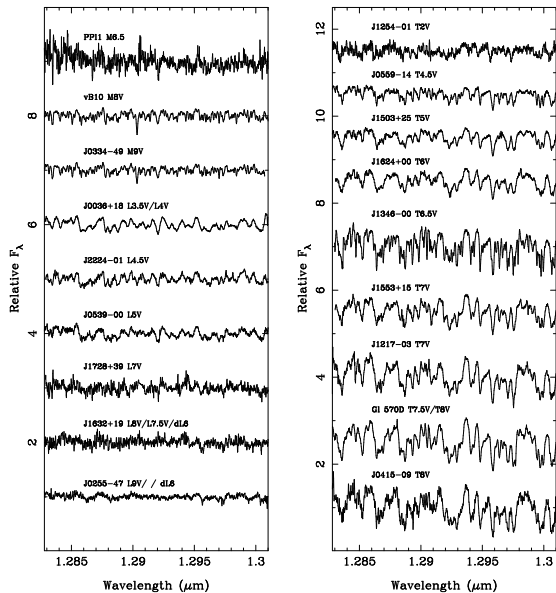


Fig. 3.— NIRSPEC spectra of our sample centered at $1.292 \mu\text{m}$. All spectra are normalized to unity and shifted in velocity to vacuum wavelengths. The spectra of the left panel are offset by 1 on the vertical axis. Data in the right panel are offset by 1 (T2V–T6V dwarfs, top four spectra) and by 1.5 (T6.5V–T8V dwarfs, bottom five spectra).

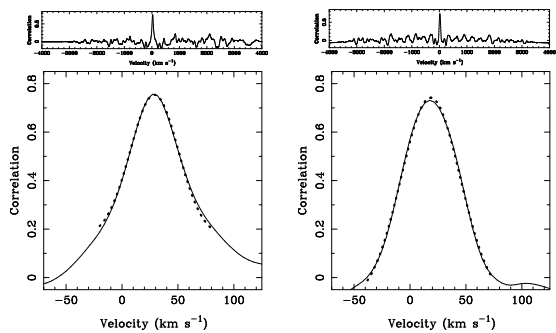


Fig. 4.— Cross-correlation functions of G1570 D against J0559–14 (left panel, spectra centered at $1.292 \mu\text{m}$), and J0036+18 against vB10 (right panel, spectra centered at $1.230 \mu\text{m}$). The bottom panels show an enlargement around the maximum peak of the cross-correlation functions (thin line) and the best Gaussian fits to the core of the peak (thick dotted line).

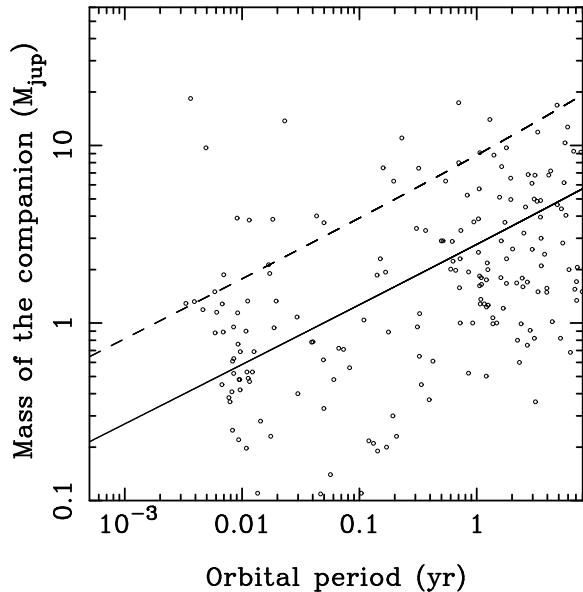


Fig. 5.— Detectability of substellar companions around the T4.5V dwarf J0559–14 using our NIRSPEC data. Companions with masses above the curves can be excluded with a confidence of $1\text{-}\sigma$ (solid line) and $3\text{-}\sigma$ (dashed line). As indicated in the text, the time coverage of our data allows us to study orbits with periods of a few days and a few years; orbits in between are not well sampled. To compute the detectability curves we have adopted circular orbits parallel to the line of sight, a mass of $0.06 M_{\odot}$ and a radial velocity amplitude of 0.5 km s^{-1} for the primary component. Known radial velocity planets around stars are plotted as open circles.

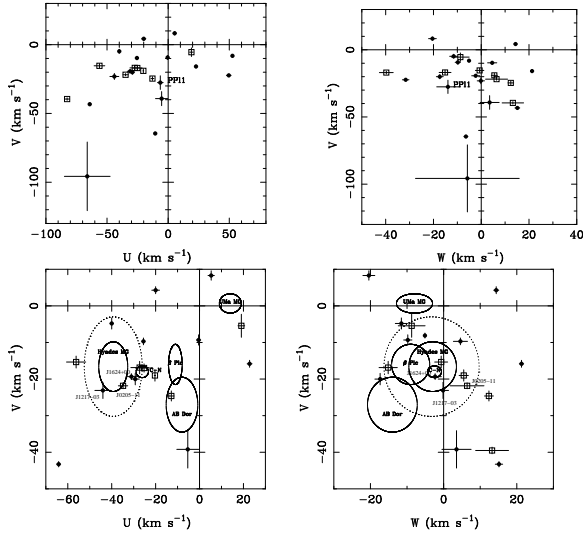


Fig. 6.— Space motions of our sample of ultra-cool dwarfs (filled circles) and the L dwarfs from the literature (open squares) with $d \leq 20$ pc. The young Pleiades brown dwarf PP11 is indicated in the top panels. An enlargement is shown in the bottom panels along with the position of various nearby star moving groups (ellipses, C-N stands for Carina-near). Solid line ellipses stand for the $1\text{-}\sigma$ location of the moving groups, and the dotted ellipse represents the $2\text{-}\sigma$ width of the Hyades moving group. The Pleiad PP11 is not included in the bottom panels.

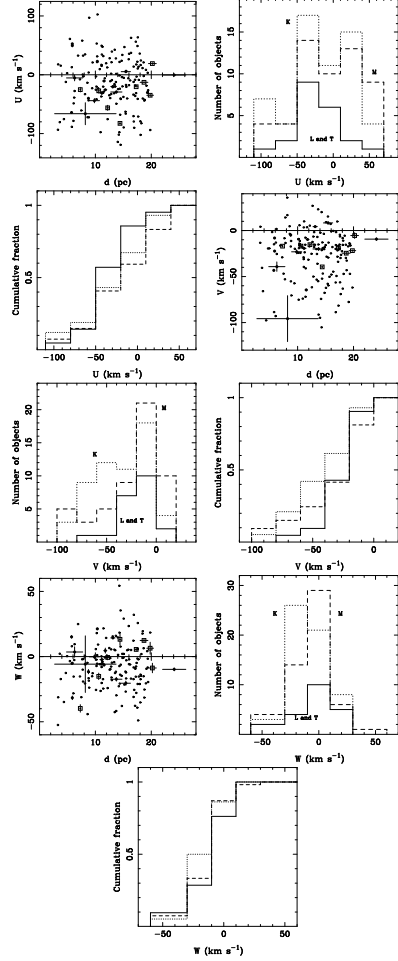


Fig. 7.— (*Left panels*). Space velocities of our sample of ultracool dwarfs (filled symbols), the extended sample (open squares), and the G, K, and M0–M5 stars (tiny circles). Only the error bars of the ultracool dwarfs are depicted for the clarity of the figure. (*Middle panels*). UVW distributions for the various populations (K stars — dotted histogram; early-M stars — dashed histogram; L and T dwarfs — solid histogram). (*Right panels*). Cumulative distributions of space velocities.

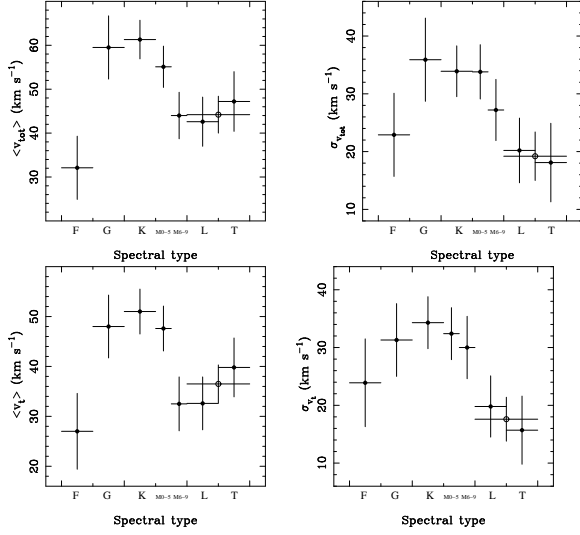


Fig. 8.— (*Left panels*) Average Galactic velocity ($\langle v_{\text{tot}} \rangle$) and tangential velocity ($\langle v_t \rangle$) as a function of spectral type. (*Right panels*) Dispersion of Galactic ($\sigma_{v_{\text{tot}}}$) and tangential (σ_{v_t}) velocities as a function of spectral type. The diagrams cover the mass interval $2\text{--}0.05 M_{\odot}$. Vertical uncertainties correspond to the error of the mean, while the horizontal error bars account for the spectral range covered by individual measurements. All data are volume-limited to ~ 20 pc. Note that we have split our sample of ultracool dwarfs into the L and T classifications (filled symbols). The open circle corresponds to the combined L and T data. The values of F-type stars may need some correction (see text).

TABLE 1
HELIOCENTRIC VELOCITIES OF OUR SAMPLE.

Object	SpT	Obs. date	MJD (−50000)	Reference object					$v_{\text{rot}} \sin i^c$ (km s ^{−1})	Previous (km s ^{−1})
				$v_B 10^a$ (km s ^{−1})	J2224−01 ^a (km s ^{−1})	J0559−14 ^a (km s ^{−1})	J1217−03 ^a (km s ^{−1})	Other ^b (km s ^{−1})		
PP11	M6.5	2005 Oct 26	3669.51110	+5.5±1.6	20.7	+15.4±1.6
vB10	M8V	2005 Oct 28	3671.51447	+5.3±1.9	+5.3±2.3	6.5 ^e	+35.0
		2001 Jun 15	2075.58951	+35.0±1.5 ^d		
DENIS-P J033411.39−495333.6	M9V	2001 Nov 02	2215.20560	+34.3±1.5 ^d	≤15	+35.2±2.0
		2005 Oct 26	3669.48071	+70.2±1.0		
2MASS J00361617+1821104	L3.5V/L4V	2005 Oct 28	3671.48317	+69.8±1.0	+69.8±1.0	36.0	
		2004 Dec 05	3344.31265	+18.2±1.6	+18.6±1.4		
2MASS J22244381−0158521	L4.5V	2005 Oct 28	3671.43118	...	+17.6±1.5	+17.7±1.0	30.7	−37.4±3.4
		2001 Jun 15	2075.61089	−37.8±1.0		
SDSS J053951.99−005902.0	L5V	2001 Nov 02	2215.45928	+11.5±2.7	+11.5±1.9	33.2	
		2005 Oct 27	3670.50549	...	+11.8±2.3	+11.3±1.8		
2MASS J17281150+3948593AB	L7V	2001 Jun 15	2075.54466	−12.2±1.7	−12.8±1.0	24.1	
2MASS J16322911+1904407	L8V/L7.5V/dL6	2001 Jun 15	2075.51675	−5.5±3.7	−5.9±2.2	21.8	+5:
DENIS-P J0255.0−4700	L9V/dL6	2005 Oct 27	3670.44084	+17.9±3.6	+17.5±2.8	+16.0±3.8	41.0	+13.0±2.0
SDSSp J125453.90−012247.4	T2V	2006 Jan 19	3754.61049	...	−0.1±5.4	+0.9±2.2	28.4	
2MASS J05591914−1404488	T4.5V	2001 Nov 02	2075.41290	−13.1±2.8	−13.8±3.7	22.8	
		2004 Dec 05	3344.54854	...	−14.6±1.3	−14.0±3.8		
		2005 Oct 26	3669.57615	...	−13.7±1.6	−13.6±1.6		
		2005 Oct 27	3670.53068	...	−14.2±1.6	−13.0±1.9		
2MASS J15031961+2525196	T5V	2005 Oct 28	3671.54024	...	−14.3±1.9	−13.8±1.0		
2MASS J15031961+2525196	T5V	2006 Jan 19	3754.66827	...	−40.1±5.8	−39.9±2.6	−40.5±2.1	...	32.1	
SDSS J162414.37+002915.6	T6V	2001 Jun 15	2075.44304	−30.7±3.0	36.6	
SDSS J134646.45−003150.4	T6.5V	2001 Jun 15	2075.34518	−23.1±1.5	≤15	
2MASS J15530228+1532369	T7V	2001 Jun 15	2075.41290	−32.8±3.3	−32.9±3.0	...	29.4	
2MASS J12171110−0311131	T7V/T8V	2001 Jun 15	2075.25577	+5.0±1.6	31.4	
GI 570D	T7.5V/T8V	2001 Jun 15	2075.38494	+28.9±2.4	+28.2±3.1	...	30.7	
2MASS J04151954−0935066	T8V	2005 Oct 26	3669.55271	+49.6±1.2	+51.0±4.3	...	33.5	

^aHeliocentric radial velocities (km s^{−1}) used in the cross-correlation: −35.0 (vB10), −37.8 (J2224−01), −13.8 (J0559−14), and +5.0 (J1217−03).

^bThe dwarf's earliest spectrum acts as the reference spectrum in the cross-correlation.

^cAverage rotational velocity from Zapatero Osorio et al. (2006).

^dHeliocentric velocity obtained from the centroids of the K1 lines.

^eRotational velocity from Mohanty & Basri (2003).

References. — (1) Martín et al. (1998); (2) Mohanty & Basri (2003); (3) Bailer-Jones (2004).

TABLE 2
MEAN HELIOCENTRIC RADIAL VELOCITIES.

Object	SpT	Δt	$\langle v_h \rangle$ (km s^{-1})	N
PP11	M6.5	2.0 d	$+5.4 \pm 1.7$	2
J0334-49	M9V	2.0 d	$+70.0 \pm 1.0$	2
J0036+18	L3.5V/L4V	0.90 yr	$+18.1 \pm 1.5$	2
J0539-00	L5V	3.98 yr	$+11.7 \pm 2.1$	2
J0559-14	T4.5V	4.37 yr	-13.8 ± 0.2^a	5

^aThe associated velocity uncertainty corresponds to the error of the mean.

TABLE 3
GALACTIC VELOCITIES OF OUR SAMPLE.

Object	SpT	d^a (pc)	$\mu_\alpha \cos \delta^a$ (mas yr^{-1})	μ_δ^a (mas yr^{-1})	U (km s^{-1})	V (km s^{-1})	W (km s^{-1})
PP11 ^b	M6.5V	133.8	+19.7	-44.8	-6.4 ± 2.3	-27.6 ± 5.0	-14.0 ± 4.7
vB 10 ^c	M8V	5.9	-578.8	-1331.6	$+52.6 \pm 0.8$	-8.1 ± 0.7	-5.1 ± 0.2
J0334-49 ^d	M9V	8.2	+2350.0	+470.0	-66.2 ± 18.7	-95.7 ± 25.0	-5.8 ± 21.7
J0036+18	L3.5V/L4V	8.8	+899.1	+120.0	-40.0 ± 0.8	-4.8 ± 1.5	-11.5 ± 1.7
J2224-01	L4.5V	11.5	+463.8	-865.8	-10.6 ± 0.6	-64.5 ± 0.9	-6.4 ± 0.8
J0539-00	L5V	13.1	+164.4	+315.9	-20.0 ± 1.8	$+4.3 \pm 1.0$	$+14.4 \pm 0.7$
J1728+39AB	L7V	24.1	+25.9	-36.8	-0.4 ± 1.0	-9.3 ± 1.4	-9.8 ± 1.1
J1632+19	L8V/L7.5V/dL6	15.4	+294.5	-56.6	$+5.3 \pm 1.4$	$+8.3 \pm 1.3$	-20.4 ± 1.6
J0255-47	L9V/dL6	6.3	+1036.6	-598.5	-5.4 ± 5.0	-39.2 ± 5.1	$+3.5 \pm 4.0$
J1254-01	T2V	11.8	-478.7	+130.1	-25.6 ± 0.8	-9.7 ± 0.9	$+4.6 \pm 1.9$
J0559-14	T4.5V	10.3	+562.1	-342.4	$+22.8 \pm 1.1$	-15.8 ± 1.0	$+21.3 \pm 0.6$
J1624+00	T6V	11.2	-378.6	-2.5	-31.0 ± 2.5	-19.3 ± 0.8	-2.3 ± 1.7
J1346-00	T6.5V	13.7	-473.1	-132.3	-29.3 ± 1.8	-20.0 ± 1.6	-17.4 ± 1.4
J1217-03	T7V/T8V	9.8	-1057.8	+91.6	-44.0 ± 3.6	-23.1 ± 2.2	-0.2 ± 1.5
G1570D ^c	T7.5V/T8V	5.9	+1034.1	-1725.5	$+49.6 \pm 2.0$	-22.3 ± 0.8	-31.6 ± 1.4
J0415-09	T8V	5.7	+2192.8	+527.3	-64.2 ± 0.9	-43.3 ± 0.7	$+15.1 \pm 1.0$

^aFrom Perryman et al. (1997); Dahn et al. (2002); Vrba et al. (2004); Knapp et al. (2004); An et al. (2007).

^bDistance and proper motion of the Pleiades cluster.

^cDistance and proper motion of the primary stars (Perryman et al. 1997).

^dSpectroscopic parallax from Phan-Bao et al. (2006).

TABLE 4
GALACTIC VELOCITIES OF AN ADDITIONAL SET OF L-TYPE DWARFS.

Object	SpT	d (pc)	$\mu_\alpha \cos \delta$ (mas yr ⁻¹)	μ_δ (mas yr ⁻¹)	v_h (km s ⁻¹)	U (km s ⁻¹)	V (km s ⁻¹)	W (km s ⁻¹)	Ref
2MASS J07464256+2000321	L0.5V	12.2	-374.044	-57.905	+54	-56.2±4.4	-15.3±1.6	-0.7±1.8	1, 3
2MASS J14392836+1929149	L1V	14.4	-1229.791	+406.714	-28	-82.6±2.1	-39.5±0.9	+13.2±4.5	1, 2, 3
Ketu 1AB	L2V	18.7	-284.790	+10.941	+17	-12.8±1.2	-24.6±1.4	+12.4±1.2	2, 3
DENIS-P J1058.7-1548	L3V	17.3	-252.931	+41.419	+19	-20.3±0.3	-19.0±1.5	+5.5±1.3	2, 3
DENIS-P J1228.2-1547AB	L5V	20.2	+133.868	-179.598	+2.5	+19.0±1.5	-5.4±3.1	-8.7±3.7	2, 3
2MASS J15074769-1627386	L5V	7.3	-161.476	-888.547	-39	-25.3±3.9	-17.0±1.1	-39.8±2.9	1, 3
DENIS-P J0205.4-1159AB	L7V	19.8	+434.348	+54.871	+7	-34.8±2.1	-21.8±0.8	+6.4±4.6	2, 3
2MASS J08251968+2115521	L7.5V	10.6	-506.522	-292.729	+20	-27.3±4.0	-16.9±1.7	-15.1±2.5	1, 3, 4

References. — Radial velocities from: (1) Bailer-Jones (2004); (2) Mohanty & Basri (2003). Distances and proper motions from: (3) Dahn et al. (2002); (4) Vrba et al. (2004).

TABLE 5
 UVW , TOTAL GALACTIC AND TANGENTIAL VELOCITY DISTRIBUTIONS OF STARS AND BROWN DWARFS
WITH $d \leq 20$ PC.

SpT	N	$\langle d \rangle^a$ (pc)	$\langle \mu \rangle^a$ (" yr ⁻¹)	σ_U (km s ⁻¹)	σ_V (km s ⁻¹)	σ_W (km s ⁻¹)	$\langle v_{\text{tot}} \rangle^a$ (km s ⁻¹)	$\langle v_t \rangle^a$ (km s ⁻¹)	Age (Gyr)	Ref.
F	10	15.4 (3.4)	0.44 (0.59)	30.9	10.3	18.1	32.1 (22.9)	27.0 (23.9)	2.2 ^{+3.0} _{-1.6}	1, 5
G	25	15.6 (3.9)	0.68 (0.82)	41.3	29.3	20.5	59.5 (35.9)	48.0 (31.3)	9.0 ^{+6.7} _{-4.5}	1, 5
K	58	14.0 (3.4)	0.78 (0.80)	43.7	32.9	15.9	61.3 (33.9)	51.0 (34.3)	7.6 ^{+3.4} _{-2.6}	1, 5
M0-M5	52	10.3 (4.0)	1.12 (1.38)	47.1	30.7	19.5	55.1 (33.8)	47.6 (32.4)	7.5 ^{+3.6} _{-2.7}	1, 5
M6-M9	31 ^b	17.4 (5.9)	0.45 (0.45)	36.5	20.6	15.7	44.0 (29.6)	32.5 (30.0)	3.8 ^{+2.8} _{-1.9}	2, 8
L and T ^c	13	10.3 (3.2)	0.92 (0.64)	30.0	19.9	15.2	43.8 (17.4)	37.5 (14.3)	0.9 ^{+1.1} _{-0.6}	2, 5-7
L and T ^d	21	12.2 (4.4)	0.77 (0.57)	30.2	16.5	15.8	44.2 (19.1)	36.5 (17.6)	1.2 ^{+1.1} _{-0.7}	2-7

^aValues in brackets correspond to the width of the distributions (or σ).

^cIncludes the 29 objects extracted from Reid et al. (2002) and the two field M dwarfs in our sample.

^cSample shown in Table 3.

^dExtended sample.

References. — Radial velocities from (1) Kharchenko (2004); (2) this paper; (3) Mohanty & Basri (2003); (4) Bailer-Jones (2004). Distances and proper motions from (5) Perryman et al. (1997); (6) Dahn et al. (2002); (7) Vrba et al. (2004); (8) Reid et al. (2002).